Ultramicroscopy 10 (1982) 55–62
North-Holland Publishing Company

FROZEN AQUEOUS SUSPENSIONS

J. DUBOCHET, J.-J. CHANG, R. FREEMAN, J. LEPAULT and A.W. McDOWALL

European Molecular Biology Laboratory, Postfach 10.2209, D-6900 Heidelberg, Fed. Rep. of Germany

Received 10 March 1982

Frozen aqueous suspensions can be observed under good conditions when the specimen is vitrified. The contrast then obtained from embedded particles is low but measurable. It can be quantitatively controlled by adjusting the composition of the solution if partial evaporation is prevented. When this is the case, contrast measurements remain within 20% of the theoretically predicted values. Three aspects of electron beam damage at low temperatures are described: (1) Beam-induced transformation of cellulose nitrate into crystals, probably of N_2O. (2) Realization of mass loss on warming organic specimens irradiated at low temperature. (3) Bubbling in vitreous ice.

1. Introduction

The recent finding that aqueous solutions can be vitrified in a form suitable for electron microscopy [1] indicates a method for overcoming freezing artefacts. We have studied methods of preparation of aqueous solutions for electron microscopy and their behaviour when irradiated by the electron beam [2]. We have also explored some of the possibilities offered for the observation of frozen hydrated biological particles [3]. In the present article we emphasize a few points mentioned previously and put forward new data concerning the observation of frozen hydrated specimens and the way they are affected by the electron beam.

2. Vitrification

Frozen hydrated specimens must be *thin* and *vitrified* for satisfactory cryo electron microscopic observation. The first of these requirements is obvious for every transmission electron microscopist; the second is illustrated in fig. 1 which shows suspensions of λ bacteriophages and polystyrene spheres, frozen under conditions where water is crystallized (A and B) and where the sample is vitrified (C and D). The large hexagonal ice crystals shown in fig. 1A are easily recognizable by the bend contours, or more precisely identified by electron diffraction (not shown). During the process of crystallization, particles are expelled from the growing ice crystals. Some of them are even pushed above the surface of the sample, thus partially losing their aqueous environment. Therefore, they have a higher contrast (arrows), sometimes comparable even to the dry sample (fig. 1E). The situation becomes worse when an aqueous solution is frozen. Solute molecules cannot be integrated into the growing water crystal. The sample is divided into pure crystalline water and a phase of concentrated solute. This is illustrated in fig. 1B by a frozen suspension of λ bacteriophages (arrows) in 30% sodium phosphotungstate.

Vitrifying water means, by definition, forming a noncrystalline solid phase which, if rewarmed above the characteristic devitrification temperature (T_v, around 135 K), undergoes a transition into crystalline ice. It has been known for a long time that vitrified water could be obtained by condensation of water vapour at low pressure onto a cold substrate [4]. We have recently found that pure water and aqueous solutions in layers thin enough for electron microscopy can also be vitrified [1]. Upon vitrification, water and solute mole-

0304-3991/82/0000–0000/$02.75

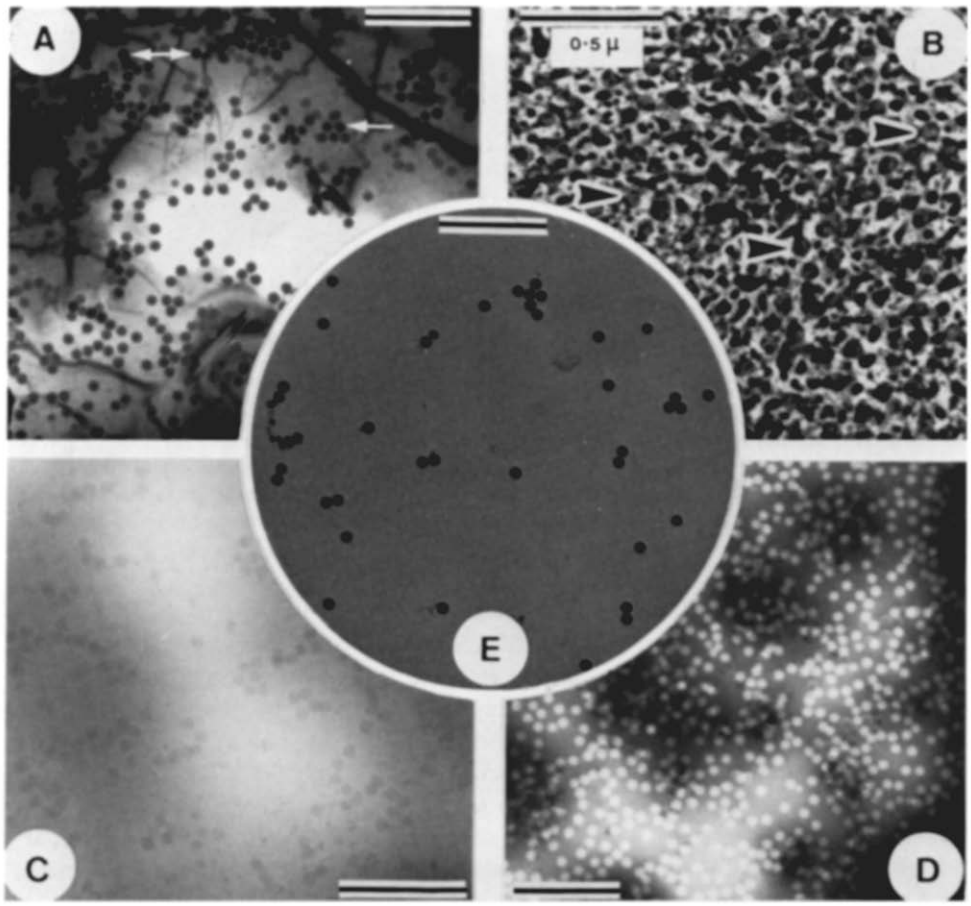

Fig. 1. Frozen-hydrated suspensions observed at 110 K with 80 kV electrons; unless otherwise stated, the bar represents 1 μm. (A) Frozen suspension of 114 nm diameter polystyrene spheres in water crystallized in large hexagonal crystals; some polystyrene spheres appear with a high contrast (arrows); original magnification: 17,000×. (B) Frozen suspension of λ bacteriophages (arrows) in 30% sodium phosphotungstate solution; water is crystallized in small cubic crystals from which the solute is excluded; original magnification: 46,000×. (C) Vitrified suspension of polystyrene sphere in pure water; original magnification: 20,000×. (D) Vitrified suspension of polystyrene sphere in 30% sodium phosphotungstate solution; original magnification: 17,000×. (e) Same preparation as in C after freeze-drying; original magnification: 17,000×.

cules and any particles in suspension are immobilized before they have time to rearrange. In fig. 1C, the polystyrene spheres display a low but positive contrast because they are scattering 7% more than vitreous ice. Replacing water by a 30% aqueous solution of sodium phosphotungstate (fig. 1D) increases the scattering of the solute by about 27%, with the result that the polystyrene spheres appear with negative contrast.

3. Contrast, mass and density

As illustrated in figs. 1C–1E, particle contrast in the vitrified sample is related to the differential scattering of the particle with its surroundings. Consequently, contrast measurements, together with the knowledge of scattering coefficients of the various constituents of the specimen, allow one to calculate the mass of each of the constituents. The scattering data of all atoms have been studied in

great detail. Unfortunately the results presented in the literature are not in a form directly usable for our purpose. In particular, long calculations are required to derive from published data the proportion of electrons scattered into a given solid angle by a unit mass thickness of water or of typical biological material. We have made these calculations and present them in a form directly usable for mass determination [5]. As a control, we compare the results obtained from direct measurements on images of polystyrene spheres with those derived from the calculations.

Polystyrene spheres consist of carbon atoms and hydrogen atoms in equal proportions. They have a density of 1.05 g cm^{-3} [6], and for the batch used in this experiment (Polysciences, Inc., Warrington, PA 18976, USA) a diameter of 114 ± 9 nm. From these data, together with those on scattering, it is calculated that of the electrons which traverse the sphere diameter, 48% are scattered outside an angle of 8.3 mrad. This corresponds to a 60 μm aperture in a Philips 400 electron microscope operating at 80 kV. Thus, it is expected that, in the bright-field image, the ratio D_1/D_2 from the number of electrons in an image element in the centre of a 114 nm polystyrene sphere to the number in an element outside the sphere is 0.52 if the sphere stands alone on a supporting film. Actual measurements give the value of 0.47 ± 0.03. The same calculation was made for an equally thick layer of vitrified ice (probable density: 0.933 g cm^{-3}) and for deuterated ice (D_2O; probable density: 1.040 g cm^{-3}) and the ratio D_1/D_2 for spheres embedded in these vitrified media calculated and compared to the measured value. Table 1 summarizes the results. It shows that values obtained from theoretical calculations agree reasonably well with those measured on the micrographs. For medium or small apertures, absolute mass measurements are reliable within 20%. The comparison between normal and deuterated water and polystyrene spheres fits also within the same error. The larger absolute error found for large aperture angles is, however, surprising.

The contrast of particles embedded in vitrified suspensions can be adjusted by the replacement of pure water by a solution of dense molecules. This is illustrated in figs. 1C and 1D. The possibilities offered by this method for contrast matching on biological specimens have been discussed elsewhere [3]. However, quantitative adjustment of contrast requires – besides the knowledge of scattering coefficients – that the concentration of the solute remains unchanged during preparation of the specimen. This is not always the case when specimens are prepared by spray freezing or by spreading on alkylamine-treated films [2]. Before the specimen is stabilized by low temperature, the water may have time to partially evaporate. In order to measure the amount of drying during preparation, we have prepared frozen hydrated

Table 1
Calculated and measured scattering data for 114 nm polystyrene spheres

Environment	Semi-aperture angle (mrad)	D_1/D_2	
		Measured	Calculated [5]
In vacuum	4.5	0.40 ± 0.04	0.43
	8.3	0.47 ± 0.03	0.52
	15.2	0.53 ± 0.02	0.66
In vitrified water	8.3	0.93 ± 0.02	0.91
In vitrified deuterated water	8.3	0.92 ± 0.02	0.91

Values for the ratio D_1/D_2 calculated or measured for a bright-field amplitude image of 114 nm diameter polystyrene spheres at 80 kV. Spheres are standing on a clean carbon film or are fully embedded in vitrified water or deuterated water.

D_1/D_2 = (electron dose received per image element in the center of the sphere)/(electron dose received per image element outside of the sphere).

samples of polystyrene spheres in heavy salt solutions and calculated the final water concentration from contrast measurements on the spheres. For specimens prepared by spray freezing, the effect of evaporation is important. Evaporation is inversely related to the size of the drops, and for small drops ($< 30\ \mu m^3$), more than 50% of the water evaporates. After spreading on alkylamine-treated films, evaporation may differ from one region of the specimen to the other. Frequently, some regions at the edges of thin layers of liquid are completely dried, but regions where evaporation is minimal are easily recognizable. In particular, this is the case for grid squares covered by a uniform layer of frozen solution. An obvious method for overcoming the effect of partial drying for quantitative contrast measurements is to include an internal standard in the suspension (for example, polystyrene spheres). A more satisfactory method is to prevent evaporation. A considerable improvement is obtained by working in a humid room ($\sim 80\%$ humidity).

4. Electron beam damage

4.1. Beam-induced crystallization of cellulose nitrate

The chemical transformations taking place during irradiation in the electron microscope and the mobility of the molecular fragments are illustrated by the beam-induced crystals formed on cellulose nitrate films (collodion) irradiated below 140 K. The crystals form after a dose of about 1000 e nm^{-2}. They appear as a dense population of small curved worm-like bodies growing in an irregular longitudinal manner. Their length rarely exceeds 100 nm. With increasing dose they stop growing, becoming more compact and roughly globular, and slowly disappearing when the accumulated dose reaches the 10^5 e nm^{-2} range. They evaporate without further irradiation when the temperature is raised above 150 K. Fig. 2A shows an area of carbon-coated collodion covered with numerous beam-induced crystals (C) produced by an irradiation of 4000 e nm^{-2}. Polystyrene spheres (P) and a hexagonal ice crystal (I_h) are also visible. Electron diffraction shows the unambiguous pattern of the crystals. In the case shown in fig. 2B, it is superimposed with the diffractogram of ice in the cubic form. Three condensed gases are known to crystallize in a form compatible with this diffractogram: α-N_2, CO_2 and N_2O, all of them forming crystals of Pa3 space group with unit cell size of 0.564, 0.558 and 0.566 nm respectively. Because nitrogen and CO_2 are expected to evaporate at lower temperature, nitrous oxide appears to be the only candidate with the required properties.

As can be inferred from the fact that most crystals are much thicker than the collodion film alone, the N_2O molecules must migrate over large distances compared to the dimension of the crystals. This movement suggests a very active model for the irradiated specimen in which not only chemical reactions take place but also where molecular fragments are diffusing over long distances. One should, however, keep in mind that under our working conditions a thin layer of vitreous ice is likely to "sandwich" the carbon–collodion supporting film. It is probable that the reaction leading to the formation of N_2O crystals does not take place on the free surface of the supporting film but at the interface between supporting film and vitreous ice. Because this fact may change crystallization and evaporation properties, our conclusion that beam-induced crystals are made out of N_2O needs confirmation.

4.2. Mass loss

When studying radiation damage by spectroscopic methods, solid state physicists have generally observed more damage at low temperature than at room temperature. They also find that some restoration may take place when the specimen, irradiated at low temperature, is warmed again. Measuring other parameters, namely the displacement of atoms or of molecular fragments, electron microscopists observe the opposite effect. Beam damage is reduced at low temperature, and there are reports that the damage after irradiation at low temperature increases further when specimens are rewarmed in the absence of irradiation [7]. We test this last point using mass loss on collodion as an indicator. For that purpose separate areas of a carbon-coated collodion film, with

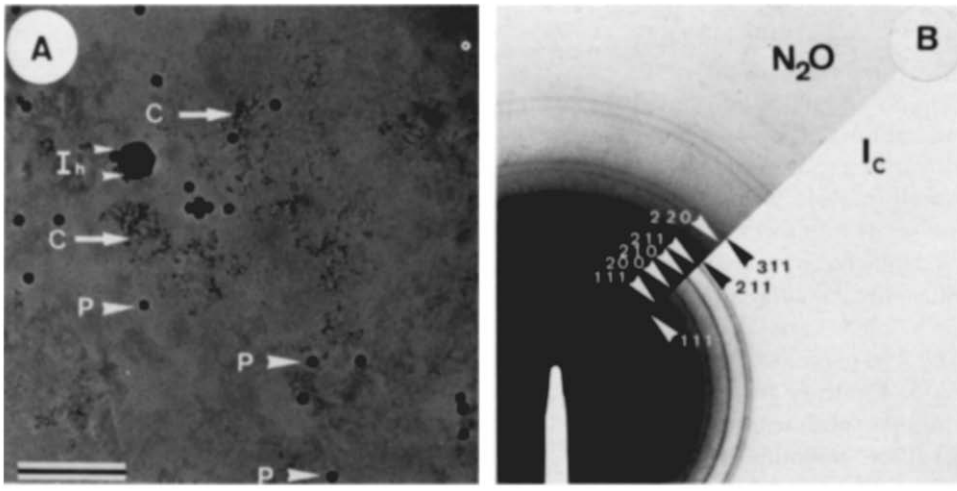

Fig. 2. (A) Beam-induced crystals (C) on carbon-coated collodion film irradiated by 4000 e nm^{-2} at 110 K; polystyrene spheres are marked P; I_h depicts a contaminating crystal of hexagonal ice (snow); the bar represents 1 μm; original magnification: 17,000×. (B) Electron diffractogram of an area similar to the one shown in (A) but also covered with a layer of cubic ice crystals (I_c); the various forms of the two types of crystals are marked; the (211) reflection of I_c corresponds to 0.224 nm.

a total mass thickness of approximately 23 mg m^{-2}, are irradiated with a range of electron doses at 110 K. The specimen is then warmed up to room temperature and mass loss determined on the various areas. The mass loss is compared with the results obtained when irradiation and measurements are made at low temperature and also when irradiation and measurements are made at room temperature. Results are given in fig. 3. They show that the same electron dose produces the same basic damage, but low temperature delays its expression in the form of mass loss. Two explanations can be proposed for this phenomenon: (1) Molecular fragments are formed during irradiation. They are volatile at room temperature but not at low temperature. They evaporate, therefore, only when the sample is rewarmed. (2) In the chain of chemical reactions following an inelastic scattering event and leading to the formation of volatile fragments, some of the steps have an activation energy too high to be overcome at low temperature. The process continues only when the specimen is warmed again, leading thus to the formation of the volatile fragments.

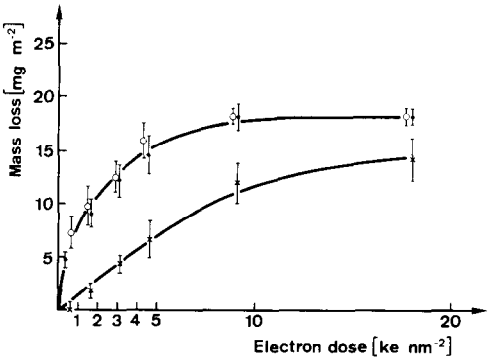

Fig. 3. Mass loss on a 25 mg m^{-2} carbon-coated collodion film irradiated by 80 kV electrons: (○) irradiation and recording at room temperature; (●) irradiation at 100 K, recording 20 min later at 260 K; (×) irradiation and recording at 100 K. Error bars indicate the standard deviation.

4.3. Bubbling

Bubbling takes place when frozen aqueous solutions of organic material are irradiated by the electron beam. It appears after some thousands of e nm^{-2}. We have interpreted it as a consequence of the accumulation of trapped volatile fragments [2]. In pure ice, bubbling appears generally after a 100-fold larger dose to a much lesser extent and

only in relatively thick layers. However, as shown in fig. 4, we have observed a remarkable bubbling phenomenon in a thick vitrified layer (in this case: 0.16 g m^{-2} corresponding to about 170 nm thickness) obtained by condensation of water vapour on a carbon-coated formvar film (polyvinylformal). The large number of small bubbles, increasing in size with increasing dose (a–d) fuse together into a large bubble (e, f) – recognizable by stereo imaging (not shown) – which breaks suddenly (f, g). After further irradiation a hole is bored completely through the specimen (h). The mass loss during the process is shown in fig. 5. Contrary to the linear relationship found on thinner specimens and when bubbling does not take place, mass loss is reproducible but follows an irregular pattern. It is very slow when the small bubbles accumulate. There is a sudden large loss when the big bubbles break, slowly followed by the continuation of the process. From this observation, we deduce that the bubbles are full of some volatile material which escapes when they break. The nature of this material is puzzling as it represents a large proportion of the total mass of the sample which originally consisted of about 90% water and only some 10% carbon and formvar. The knowledge of the chemistry occurring within the bubbles would be an important contribution to the precise understanding of beam damage.

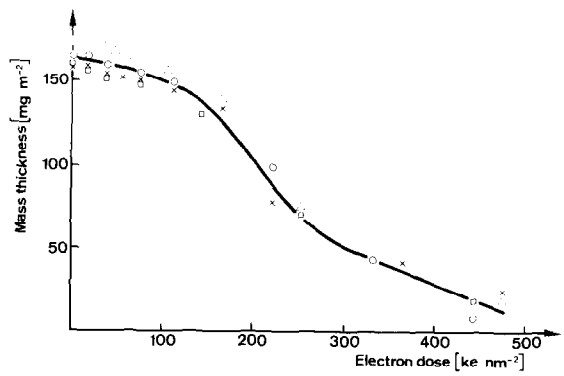

Fig. 5. Mass loss on the specimen shown in fig. 4. The heavy line is the average value deduced from 8 sets of measurements. The four sets of measurements are marked by different symbols.

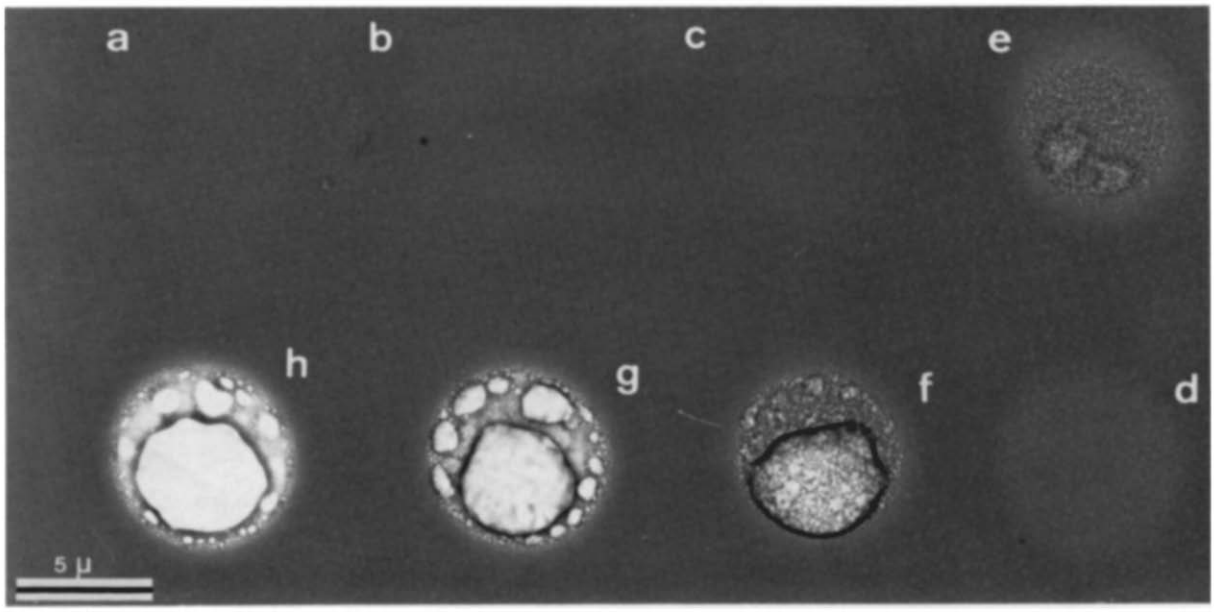

Fig. 4. Bubbling in vitrified water. A specimen of 0.160 g m^{-2} vitreous water obtained by condensation of low pressure vapour on a cold carbon-coated formvar film is irradiated at 110 K in the areas a–h by electron doses of 5, 20, 40, 80, 120, 240, 340 and 450 ke nm^{-2}, respectively, applied at the rate of 2 ke nm^{-2} s^{-1} with 80 kV electrons. Original magnification 3400×.

Acknowledgement

We thank Dr. G.J. Tatlock for his help with the determination of the nature of the beam-induced crystals, and Dr. K. Zierold for reviewing the manuscript.

References

[1] J. Dubochet and A.W. McDowall, J. Microscopy 124 (1981) RP3-4.
[2] J. Dubochet, J. Lepault, R. Freeman, J.A. Berriman and J.-C. Homo, J. Microscopy, in press.
[3] J. Lepault, F.P. Booy and J. Dubochet, J. Microscopy, in press.
[4] E.F. Burton and W.F. Oliver, Proc. Roy. Soc. (London) A153 (1935) 166.
[5] R. Eusemann, H. Rose and J. Dubochet, J. Microscopy, in press.
[6] D. Karamata, J. Ultrastruct. Res. 35 (1971) 201.
[7] G. Siegel, Z. Naturforsch. 27a (1972) 325.